

# Dirac-Proca stars

Tian-Xiang Ma, Chen Liang, Ji-Rong Ren, and Yong-Qiang Wang<sup>a</sup>

<sup>1</sup>*Key Laboratory of Quantum Theory and Applications of MoE,*

*Lanzhou Center for Theoretical Physics,*

*Lanzhou University, Lanzhou 730000, China*

<sup>2</sup>*Key Laboratory of Theoretical Physics of Gansu Province,*

*Institute of Theoretical Physics & Research Center of Gravitation,*

*Lanzhou University, Lanzhou 730000, China*

<sup>3</sup>*School of Physical Science and Technology,*

*Lanzhou University, Lanzhou 730000, China*

## Abstract

We consider a model consists of the Einstein gravity in four-dimensional spacetime, a Proca field and two Dirac fields through minimum coupling. By numerically solving this model, we obtain two types of solutions: synchronized frequency solutions and non-synchronized frequency solutions. We find that in the case of two kinds of matter fields, different families of solutions can be obtained in both synchronized and non-synchronized frequency cases, and the two families can shift to each other when certain parameters are changed. Moreover, we calculate the binding energy of multi-field solutions and give the relationship between binding energy  $E$  and synchronized frequency  $\tilde{\omega}$  (non-synchronized frequency  $\tilde{\omega}_P$ ), so as to analyze the stability of the corresponding family.

---

<sup>a</sup> yqwang@lzu.edu.cn, corresponding author

## I. INTRODUCTION

Unlike fermions that make up ordinary matter and must satisfy the Pauli exclusion principle, bosons are particles that can occupy the same quantum state. This means that bosons can form very dense and compact objects that are held together by their own gravity and quantum pressure. Among these compact objects, the macroscopic Bose-Einstein condensate formed by bosons is called a boson star [1]. Generally speaking, they do not emit any electromagnetic radiation, nor do they have a surface or event horizon. Apart from the gravitational influence on the surrounding environment, they are basically invisible. It is precisely because of their characteristic that they are difficult to interact with ordinary matter except for gravity that boson stars have become one of the important candidates for dark matter [2–6]. So far, there is no direct evidence indicating the existence of boson stars, but there are still some methods that can be used to detect them. Even if boson stars have no observable effects in the electromagnetic aspect, they are still macroscopic objects formed by gravitational interactions, so they can be indirectly observed by the gravitational lensing effect that distorts the images of background light sources such as stars or galaxies [7–9]. Moreover, with the rapid development of gravitational wave observation technology in recent decades, instruments such as LIGO and Virgo may be able to detect the characteristic signals of gravitational waves generated by boson stars when they merge with each other or with black holes [10–12], and the analysis of these gravitational wave signals also helps us to further understand the nature of boson stars.

After the classical boson star model, extended research was carried out in many different directions, one of which was to try to obtain different properties and mass upper bounds by changing the composition of the matter field. In addition to the classical boson star model composed of scalar fields [1, 13–19], there are also Dirac stars composed of spinor fields [20–24] (spin 1/2) and Proca stars composed of massive vector fields [25–29] (spin 1). Dirac stars are quantum entities consist of spinor fields, which to some extent represent the attempt of quantum gravity theory to unify gravity and quantum mechanics, and may thereby reveal some new aspects of the nature of spacetime. However, it is not particularly noteworthy in the field of astronomy. Proca stars consist of massive vector fields with spin 1, whose intrinsic angular momentum is one unit. They behave similarly to boson stars. Since Proca fields can also form stable structures, Proca stars have been widely studied in cosmology

and astrophysics, such as for simulating black hole shadows [30, 31]. They can also explain some gravitational wave events [32–34], such as GW190521. Some researchers believe that this event may be the merger of two Proca stars, rather than two black holes, because the initial mass of the objects was too large to be explained by stellar evolution [35, 36].

Apart from changing the spin of particles that make up a boson star, there are also some boson star models composed of scalar fields in different states called multi-state boson star [37, 38]. Following the study of multi-state boson stars, it was found that coupling gravity with multiple different fields can lead to soliton solutions that vary from those in the single-field case [39–41, 46–55], for example, Adding Yang-Mills fields [43–45], Maxwell fields [41, 42], axion fields [39, 53, 54], Higgs bosons [55], or superposing multiple same fields to form new configurations, such as star chains [49, 50, 52],  $\ell$ -boson stars [46]. This led to the development of multi-field boson star solutions obtained by coupling gravity with multiple fields of different spins, including solutions composed of Dirac fields and scalar fields [56] or scalar fields and Proca fields [57, 58]. So far, multi-field boson star solutions without scalar fields have not been thoroughly studied. However, considering Dirac-Proca star(DPS) model that uses Dirac fields and Proca fields coupled with gravity after excluding the scalar field components which make up traditional boson stars may have peculiar properties and stability conditions than single-state boson stars, and they may also have distinctive observational effects on dark matter and gravitational waves. Our work is to numerically solve the spherical symmetric model of two Dirac fields and one Proca field under the minimum coupling of Einstein gravity and obtain the properties of different families of solutions. All bosonic fields are in their ground state.

The structure of this paper is as follows. Sec. II introduces the basic framework and motion equations of the Einstein-Dirac-Proca system. In Sec. III, we derive the boundary conditions that each unknown function in the equation satisfies. In Sec. IV, we present numerical results of the DPSs solutions and analyze their stability. In Sec. V, We present a summary and outlook.

## II. THE MODEL SETUP

The action of the minimal coupling of Einstein gravity with one Proca field and two Dirac fields is given by

$$S = \int \sqrt{-g} d^4x \left( \frac{R}{16\pi G_0} + \mathcal{L}_D + \mathcal{L}_P \right), \quad (1)$$

where  $G_0$  is the gravitational constant,  $R$  is the scalar curvature, the Lagrangian of the Dirac field and the Proca field,  $\mathcal{L}_D$  and  $\mathcal{L}_P$ , their specific forms are

$$\mathcal{L}_D = -i \sum_{k=1}^2 \left[ \frac{1}{2} \left( \hat{D}_\mu \bar{\Psi}^{(k)} \gamma^\mu \Psi^{(k)} - \bar{\Psi}^{(k)} \gamma^\mu \hat{D}_\mu \Psi^{(k)} \right) + \mu_D \bar{\Psi}^{(k)} \Psi^{(k)} \right], \quad (2)$$

$$\mathcal{L}_P = -\frac{1}{4} \mathcal{F}_{\alpha\beta} \bar{\mathcal{F}}^{\alpha\beta} - \frac{1}{2} \mu_P^2 \mathcal{A}_\alpha \bar{\mathcal{A}}^\alpha, \quad (3)$$

where  $\Psi^{(k)}$  are spinors with mass  $\mu_D$  and  $\mathcal{A}$  is Proca field,  $\bar{\Psi}^{(k)}$  and  $\bar{\mathcal{A}}$  are complex conjugates of their corresponding fields,  $\mathcal{F} = d\mathcal{A}$ .

The equations of motion derived from the action reads

$$R_{\alpha\beta} - \frac{1}{2} g_{\alpha\beta} R = 8\pi G_0 (T_{\alpha\beta(D)} + T_{\alpha\beta(P)}), \quad (4)$$

$$\gamma^\mu \hat{D}_\mu \Psi^{(k)} - \mu_D \Psi^{(k)} = 0, \quad (5)$$

$$\nabla_\alpha \mathcal{F}^{\alpha\beta} - \mu_P^2 \mathcal{A}^\beta = 0. \quad (6)$$

where  $T_{\alpha\beta}$  is the energy-stress tensor, which has the form

$$T_{\alpha\beta(D)} = \sum_{k=1}^2 -\frac{i}{4} \left( \bar{\Psi}^{(k)} \gamma_\alpha \hat{D}_\beta \Psi^{(k)} + \bar{\Psi}^{(k)} \gamma_\beta \hat{D}_\alpha \Psi^{(k)} - \hat{D}_\alpha \bar{\Psi}^{(k)} \gamma_\beta \Psi^{(k)} - \hat{D}_\beta \bar{\Psi}^{(k)} \gamma_\alpha \Psi^{(k)} \right),$$

$$T_{\alpha\beta(P)} = \frac{1}{2} (\mathcal{F}_{\alpha\sigma} \bar{\mathcal{F}}_{\beta\gamma} + \bar{\mathcal{F}}_{\alpha\sigma} \mathcal{F}_{\beta\gamma}) g^{\sigma\gamma} - \frac{1}{4} g_{\alpha\beta} \mathcal{F}_{\sigma\tau} \bar{\mathcal{F}}^{\sigma\tau} + \frac{1}{2} \mu_P^2 [\mathcal{A}_\alpha \bar{\mathcal{A}}_\beta + \bar{\mathcal{A}}_\alpha \mathcal{A}_\beta - g_{\alpha\beta} \mathcal{A}_\sigma \bar{\mathcal{A}}^\sigma].$$

The action (1) is invariant under global  $U(1)$  transformations  $\Psi^{(k)} \rightarrow e^{i\alpha} \Psi^{(k)}$  and  $\mathcal{A}^\beta \rightarrow e^{i\alpha} \mathcal{A}^\beta$  with a constant  $\alpha$ , which means that there is a conserved current  $J^\alpha$  for this system.

$$J_D^\alpha = \bar{\Psi} \gamma^\alpha \Psi, \quad (7)$$

$$J_P^\alpha = \frac{i}{2} \left[ \bar{\mathcal{F}}^{\alpha\beta} \mathcal{A}_\beta - \mathcal{F}^{\alpha\beta} \bar{\mathcal{A}}_\beta \right]. \quad (8)$$

Integrating the time component of this four-dimensional current over a spacelike hypersurface  $\Sigma$  gives the conserved Noether charge  $Q$

$$Q_D = \int_\Sigma J_D^t, \quad Q_P = \int_\Sigma J_P^t, \quad (9)$$



This conserved charge corresponds to the particle number of the respective matter fields.

To obtain spherically symmetric solutions, we use the following form of spherically symmetric metric:

$$ds^2 = -N(r)\sigma^2(r)dt^2 + \frac{dr^2}{N(r)} + r^2 (d\theta^2 + \sin^2\theta d\varphi^2), \quad (10)$$

where  $N(r) = 1 - 2m(r)/r$ . The two pairs of Dirac fields are given by [59]:

$$\Psi^{(1)} = \begin{pmatrix} \cos(\frac{\theta}{2})[(1+i)f(r) - (1-i)g(r)] \\ i \sin(\frac{\theta}{2})[(1-i)f(r) - (1+i)g(r)] \\ -i \cos(\frac{\theta}{2})[(1-i)f(r) - (1+i)g(r)] \\ -\sin(\frac{\theta}{2})[(1+i)f(r) - (1-i)g(r)] \end{pmatrix} e^{i\frac{\varphi}{2} - i\omega_D t}, \quad (11)$$

$$\Psi^{(2)} = \begin{pmatrix} i \sin(\frac{\theta}{2})[(1+i)f(r) - (1-i)g(r)] \\ \cos(\frac{\theta}{2})[(1-i)f(r) - (1+i)g(r)] \\ \sin(\frac{\theta}{2})[(1-i)f(r) - (1+i)g(r)] \\ i \cos(\frac{\theta}{2})[(1+i)f(r) - (1-i)g(r)] \end{pmatrix} e^{-i\frac{\varphi}{2} - i\omega_D t}, \quad (12)$$

and the Proca field is

$$\mathcal{A} = [F(r)dt + iG(r)dr]e^{-i\omega_P t} \quad (13)$$

Substituting the above ansatz into the field equations (4–6) yields the following system of ordinary differential equations:

$$f' + \left( \frac{N'}{4N} + \frac{\sigma'}{2\sigma} + \frac{1}{r\sqrt{N}} + \frac{1}{r} \right) f + \left( \frac{\mu}{\sqrt{N}} - \frac{\omega_D}{N\sigma} \right) g = 0, \quad (14)$$

$$g' + \left( \frac{N'}{4N} + \frac{\sigma'}{2\sigma} - \frac{1}{r\sqrt{N}} + \frac{1}{r} \right) g + \left( \frac{\mu}{\sqrt{N}} + \frac{\omega_D}{N\sigma} \right) f = 0, \quad (15)$$

$$\frac{d}{dr} \left\{ \frac{r^2 [F' - \omega_P G]}{\sigma} \right\} = \frac{\mu_P^2 r^2 F}{\sigma N}, \quad (16)$$

$$\omega_P G - F' = \frac{\mu_P^2 \sigma^2 N G}{\omega_P}, \quad (17)$$

$$m' = \frac{32\pi G_0 r^2 \omega_D (f^2 + g^2)}{\sqrt{N}\sigma} + 4\pi G_0 r^2 \left[ \frac{(F' - \omega_P G)^2}{2\sigma^2} + \frac{\mu_P^2}{2} \left( G^2 N + \frac{F^2}{N\sigma^2} \right) \right], \quad (18)$$

$$\frac{\sigma'}{\sigma} = \frac{32\pi G_0 r}{\sqrt{N}} \left[ g f' - f g' + \frac{\omega_D (f^2 + g^2)}{N\sigma} \right] + 4\pi G_0 r \mu_P^2 \left( G^2 + \frac{F^2}{N^2 \sigma^2} \right), \quad (19)$$

The specific form of the Noether charge is:

$$Q_D = 16\pi \int_0^\infty r^2 \frac{f^2 + g^2}{\sqrt{N}} dr, \quad Q_P = 4\pi \int_0^\infty r^2 \frac{(\omega_P G - F') G}{\sigma} dr. \quad (20)$$

### III. BOUNDARY CONDITIONS

To solve the system of ordinary differential equations derived in the previous section, we have to specify the boundary conditions for each unknown function. Since they are solutions with asymptotic flatness, the metric functions  $m(r)$  and  $\sigma(r)$  have to satisfy the following boundary conditions:

$$m(0) = 0, \quad \sigma(0) = \sigma_0, \quad m(\infty) = M, \quad \sigma(\infty) = 1, \quad (21)$$

where the ADM mass  $M$  and  $\sigma_0$  are unknown constants. In addition, the matter field should vanish at infinity:

$$f(\infty) = 0, \quad g(\infty) = 0, \quad F(\infty) = 0, \quad G(\infty) = 0. \quad (22)$$

Expanding equations (14–17) near the origin, we obtain that the field functions satisfy the following condition at the origin:

$$f(0) = 0, \quad \left. \frac{dg(r)}{dr} \right|_{r=0} = 0, \quad \left. \frac{dF(r)}{dr} \right|_{r=0} = 0, \quad G(0) = 0. \quad (23)$$

### IV. NUMERICAL RESULTS

To facilitate numerical calculations, we use dimensionless quantities:

$$\begin{aligned} \tilde{r} \rightarrow r/\rho, \quad f \rightarrow \frac{\sqrt{4\pi\rho}}{M_{Pl}} f, \quad g \rightarrow \frac{\sqrt{4\pi\rho}}{M_{Pl}} g, \quad \tilde{\omega}_D \rightarrow \omega_D \rho, \quad \tilde{\mu}_D \rightarrow \mu_D \rho, \\ \tilde{F} \rightarrow \frac{\sqrt{4\pi}}{M_{Pl}} F, \quad \tilde{G} \rightarrow \frac{\sqrt{4\pi}}{M_{Pl}} G, \quad \tilde{\omega}_P \rightarrow \omega_P \rho, \quad \tilde{\mu}_P \rightarrow \mu_P \rho, \end{aligned} \quad (24)$$

where  $M_{Pl} = 1/\sqrt{G_0}$  is the Planck mass.  $\rho$  is a positive constant whose dimension is length, we let the constant  $\rho$  be  $1/\mu_S$ . Additionally, we introduce a new radial variable  $x$ :

$$x = \frac{\tilde{r}}{1 + \tilde{r}}, \quad (25)$$

where the radial coordinate  $\tilde{r} \in [0, \infty)$ , so  $x \in [0, 1]$ . We utilize the finite element method to numerically solve the system of differential equations. The integration region  $0 \leq x \leq 1$  is discretized into 1000 grid points. The Newton-Raphson method is employed as our iterative approach. To ensure the accuracy of the computational results, we enforce a relative error criterion of less than  $10^{-5}$ .

To ensure the correctness of our numerical calculations, we need to check the numerical precision by validating physical constraints [60, 61], besides using the numerical analysis methods mentioned before. In this study, we compared the asymptotic mass and the Komar mass of the electron in the numerical solution, and found that the difference between them was always less than  $10^{-5}$ .

In our model, the ground state Dirac field functions  $f$  and  $g$  have no nodes in the radial direction, so they are denoted by  $D_0$  where the subscript is the total number of radial nodes of the field functions. The ground state field functions  $F$  and  $G$  of Proca field have one node in the radial direction, so they are denoted by  $P_1$ , where the subscript has the same meaning as that of the scalar field. Therefore, in this model we use  $D_0P_1$  to represent the coexisting state of the Dirac field and Proca field. Next, we analyze the different classes of families of solutions of Dirac-Proca stars in detail.

### A. Synchronized frequency

We found through the analysis of numerical calculations that by changing the Proca field mass  $\tilde{\mu}_P$  in the synchronized frequency solutions ( $\tilde{\omega} = \tilde{\omega}_D = \tilde{\omega}_P$ ), different DPS solutions can be obtained. According to the different behaviors of the solutions at the extreme value of the synchronized frequency  $\tilde{\omega}$ , we can divide the synchronized frequency solutions into two categories:  $D$ - $P$  and  $P$ - $P$ . For  $0.828 \leq \tilde{\mu}_P \leq 0.856$ , the DPS solutions belong to the  $P$ - $P$  family; for  $0.857 < \tilde{\mu}_P \leq 0.985$ , the DPS solutions belong to the  $D$ - $P$  family. Next, we discuss in detail the properties of these two types of solutions.

#### 1. $P$ - $P$ family

The first type of synchronized frequency solutions can be obtained when the value of  $\tilde{\mu}_P$  is small. Since the two endpoints of the solution's ADM curve fall on the single-field curve of the Proca field, we call it a  $P$ - $P$  solution. When the synchronized frequency  $\tilde{\omega}$  takes the minimum or maximum value, the Dirac field disappears, and the multi-field solution becomes a single-field solution with only Proca field components. Fig. 1 shows the field functions at different synchronized frequencies  $\tilde{\omega}$ . The top two graphs are Dirac field functions ( $f$  and  $g$ ), and the bottom two graphs are Proca field functions ( $F$  and  $G$ ). It can be seen that

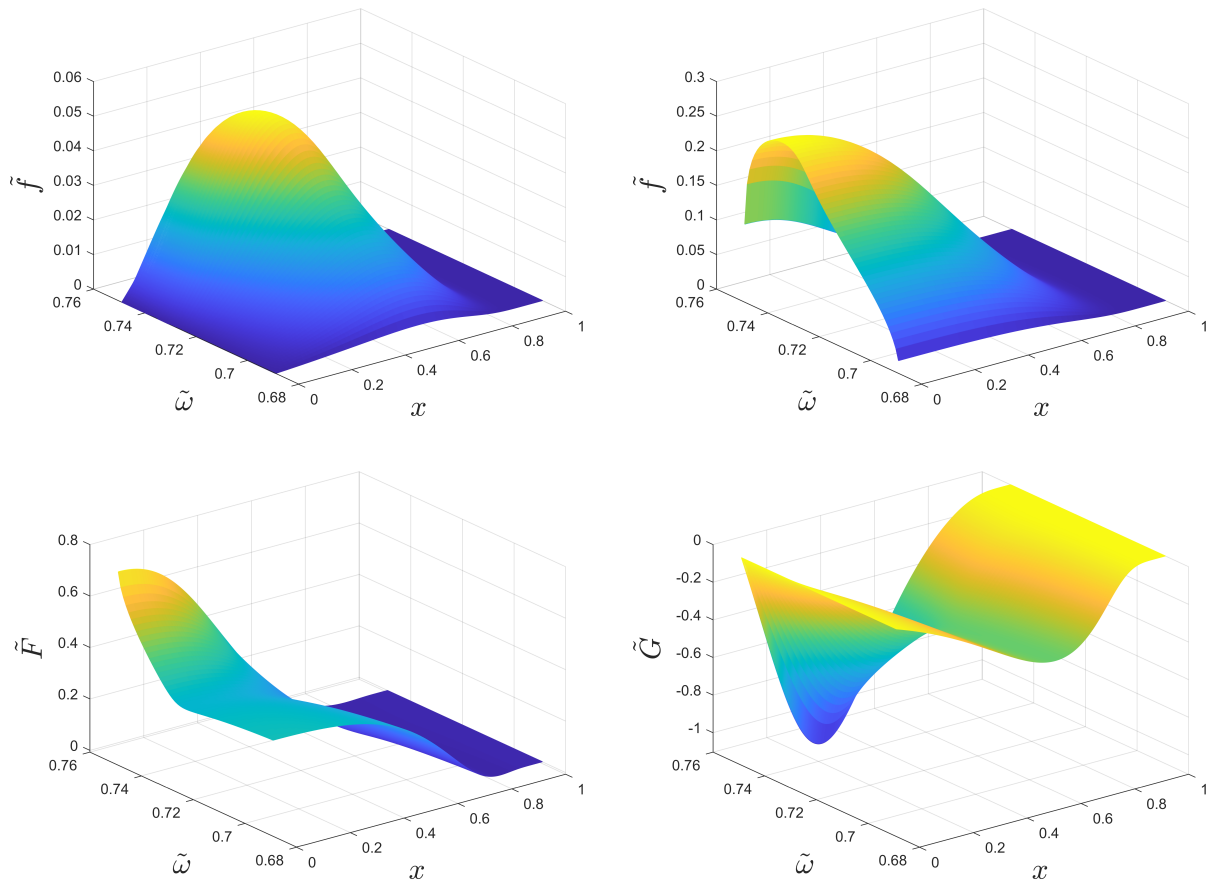


FIG. 1. The matter field functions  $\tilde{f}$ ,  $\tilde{g}$ ,  $\tilde{F}$  and  $\tilde{G}$  as functions of  $x$  and  $\tilde{\omega}$  for  $\tilde{\mu}_P = 0.845$ . All of them are in the first branch.

except for the image of  $F$  having one node, all other field functions do not have nodes. It is easy to see from the Fig. 1 that the peak absolute value of the Dirac field function in the  $P$ - $P$  family does not monotonically change with  $\tilde{\omega}$ ,  $|f_{max}|$  and  $|g_{max}|$  both exhibit a trend of increasing first and then decreasing as  $\tilde{\omega}$  increases. For Proca field,  $|F_{max}|$  and  $|G_{max}|$  increase monotonically with  $\tilde{\omega}$ .

Next, let's analyze the ADM mass of the multi-field solution. By changing the value of  $\tilde{\mu}_P$  within a certain range, we can obtain different  $P$ - $P$  solutions. The relationship between their ADM mass and the synchronized frequency  $\tilde{\omega}$  is shown in Fig. 2. The black dashed line represents the ground state Dirac field ( $D_0$ ), the red dashed line represents the Proca field ( $P_1$ ), and the blue solid line represents the multi-field solutions ( $D_0P_1$ ). We can see from this that the  $P$ - $P$  solutions have the characteristic that both ends of the multi-field

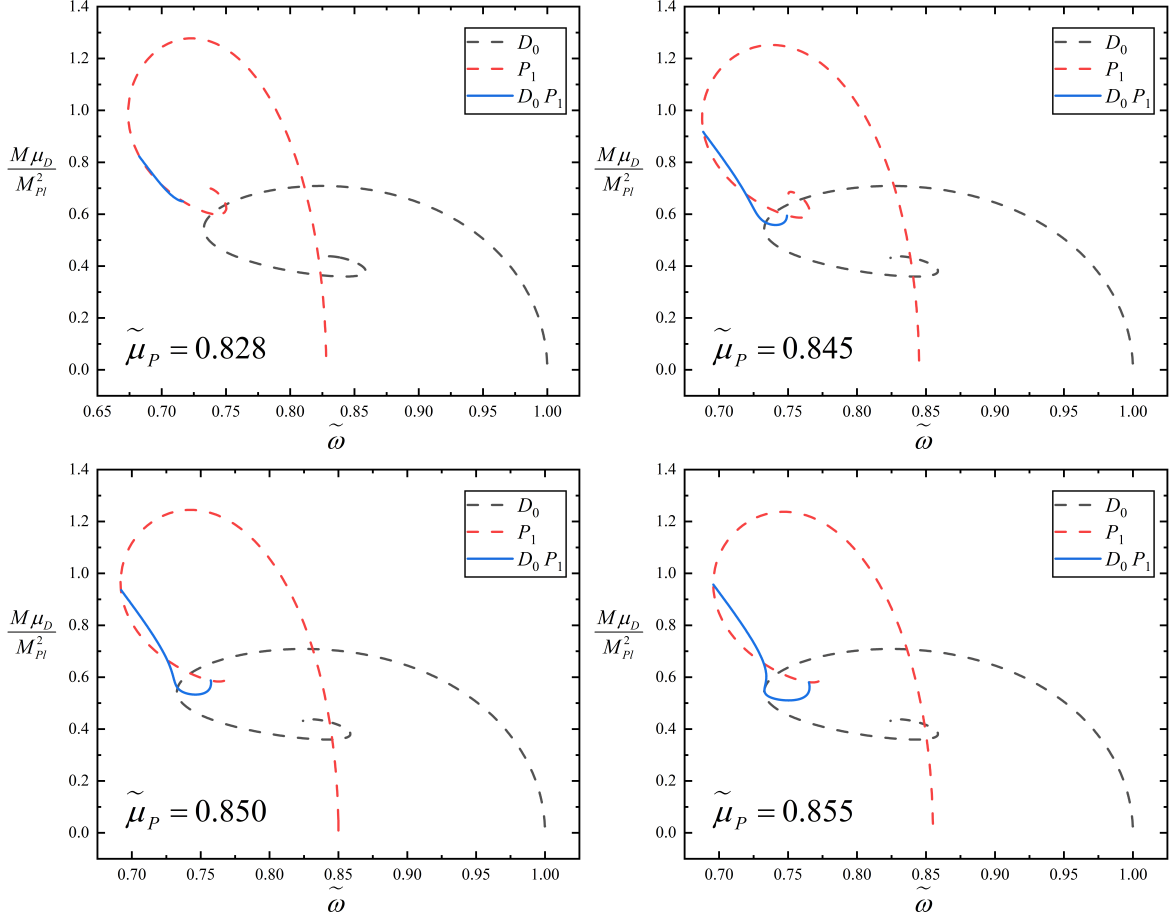


FIG. 2. The ADM mass  $M$  of the DPSs as a function of the synchronized frequency  $\tilde{\omega}$  for several values of  $\tilde{\mu}_P$ .

solutions fall on the Proca field curve. Their shape is like a spoon. With increasing  $\tilde{\mu}_P$ , the existence domain of the multi-field solutions gradually increases, and there will be a certain degree of distortion at the connection between the "spoon head" and the "spoon handle". In this domain, the ADM mass changes from a single-valued function of  $\tilde{\omega}$  to a multi-valued function. The curve starts from the Proca field and gradually extends to the right. At this time, the proportion of Dirac field component increases gradually from 0 and then decreases gradually. Finally, it terminates at another position on the Proca field, and the Dirac field disappears again.

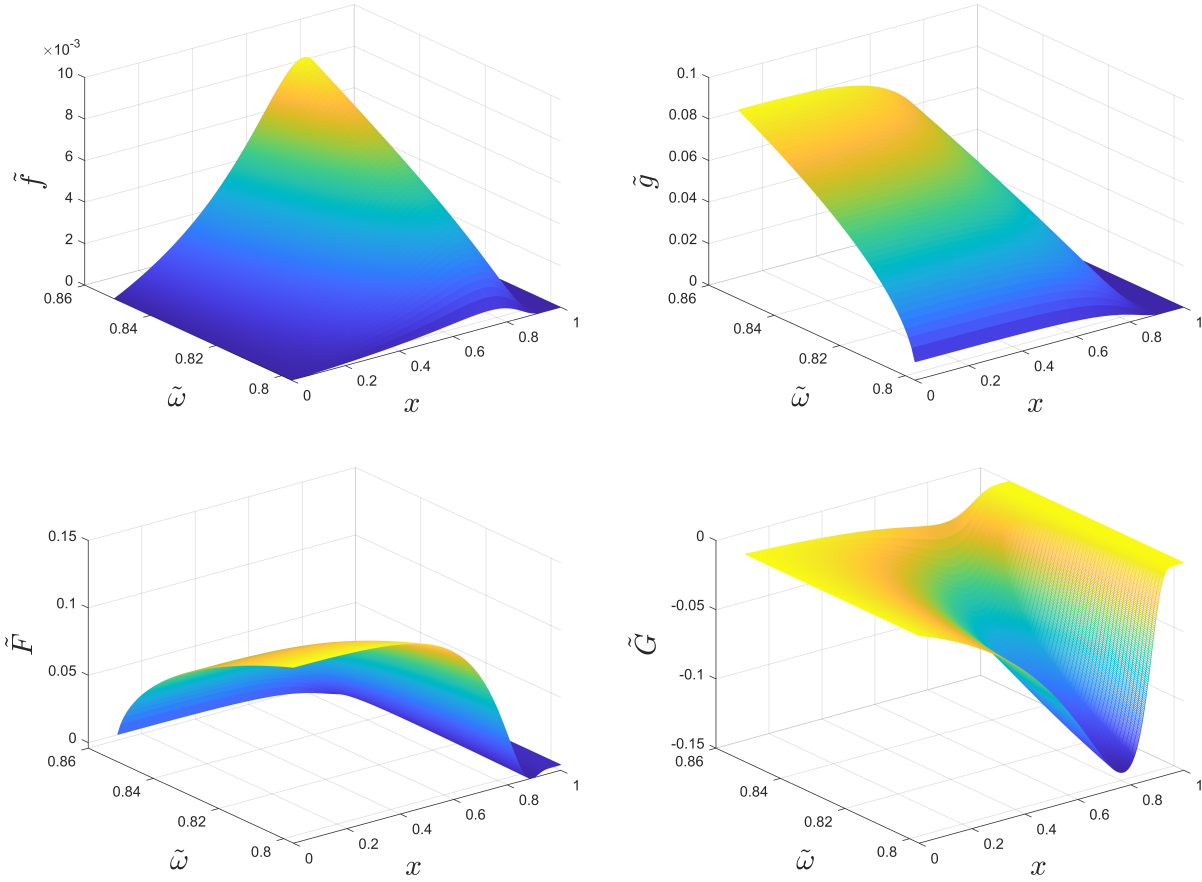


FIG. 3. The matter functions  $\tilde{f}$ ,  $\tilde{g}$ ,  $\tilde{F}$  and  $\tilde{G}$  as functions of  $x$  and  $\tilde{\omega}$  for  $\tilde{\mu}_P = 0.93$ .

## 2. $D$ - $P$ family

Next, we study the  $D$ - $P$  solutions. This family of solutions is much simpler than the  $P$ - $P$  family discussed above. The left and right ends of the  $D$ - $P$  solutions intersect with the Proca field curve and the Dirac field curve, respectively. That is, when the synchronized frequency  $\tilde{\omega}$  takes the minimum value, the Dirac field disappears, and the multi-field solution becomes a single-field solution with only Proca field components; when the synchronized frequency  $\tilde{\omega}$  takes the maximum value, the Proca field disappears, and the multi-field solution becomes a single-field solution with only Dirac field components. Moreover, compared with the  $P$ - $P$  solution, there is no distortion in the the ADM mass curve of the  $D$ - $P$  family.

Fig. 3 shows the field functions of the  $D$ - $P$  solutions at different synchronized frequencies  $\tilde{\omega}$ . The top two graphs are Dirac field functions ( $f$  and  $g$ ), and the bottom two graphs are

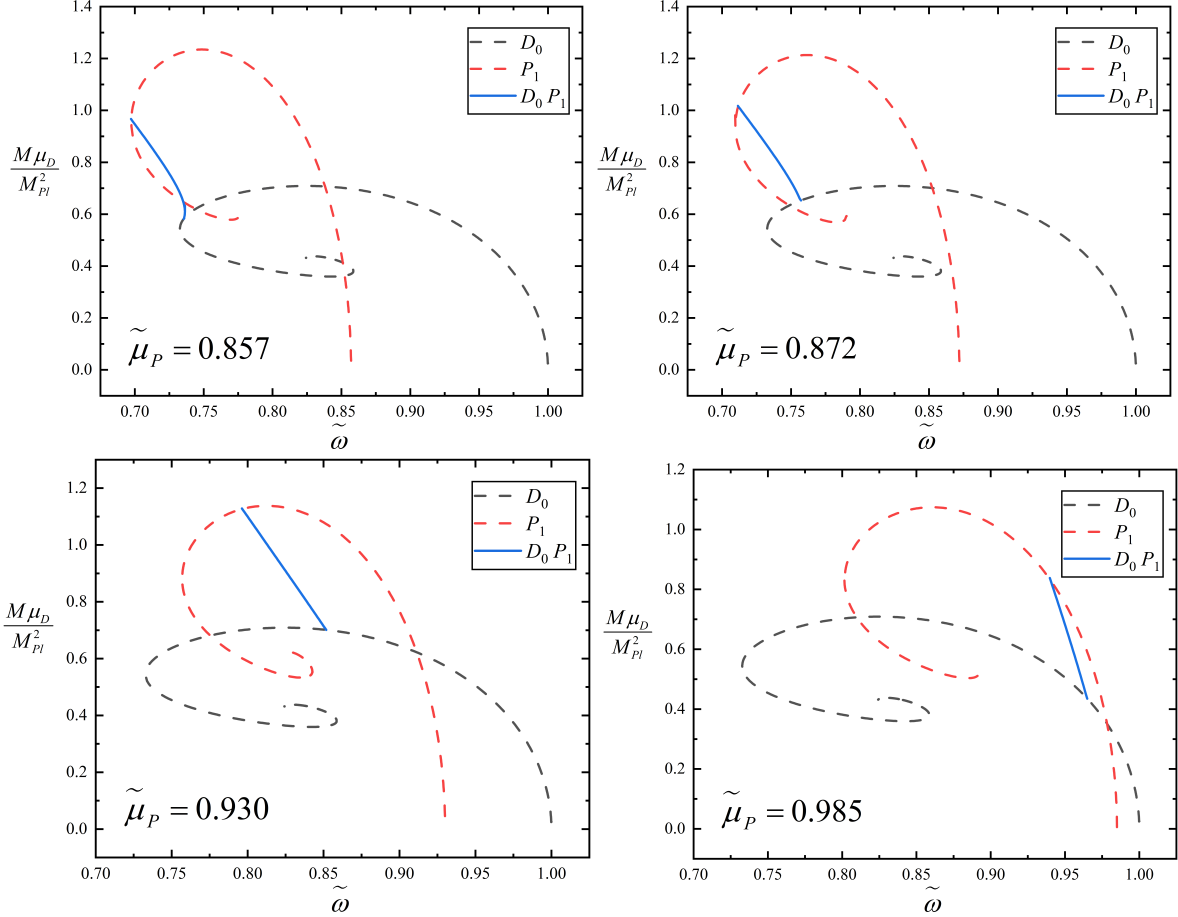


FIG. 4. The ADM mass  $M$  of the DPSs as a function of the synchronized frequency  $\tilde{\omega}$  for several values of  $\tilde{\mu}_P$ .

Proca field functions ( $F$  and  $G$ ). For  $D$ - $P$  family,  $|f_{max}|$  and  $|g_{max}|$  increase monotonically with  $\tilde{\omega}$ , and  $|F_{max}|$  and  $|G_{max}|$  decrease monotonically with  $\tilde{\omega}$ . Due to this characteristic of the  $D$ - $P$  solution, they cannot keep a certain field from disappearing as the synchronized frequency  $\tilde{\omega}$  changes.

Fig. 4 shows the relationship between the ADM mass of different  $D$ - $P$  solutions and the synchronized frequency  $\tilde{\omega}$ . Similar to the  $P$ - $P$  solution, different solutions here are still obtained by changing the parameter  $\tilde{\mu}_P$ . The  $D$ - $P$  family is similar to the single-branch solution in Ref. [56]. With increasing  $\tilde{\mu}_P$ , the  $D$ - $P$  solutions gradually move to the right, and its existence domain gradually become smaller until no solution can be found.

## B. Nonsynchronized frequency

In this section, we discuss the non-synchronized frequency solutions ( $\tilde{\omega}_D \neq \tilde{\omega}_P$ ). In order to study the influence of parameter changes on the properties of the solution, we fix  $\tilde{\mu}_D = \tilde{\mu}_P = 1$  and obtain a series of solutions by changing  $\tilde{\omega}_D$ . Similar to the synchronized frequency solutions in the previous section, we still divide it into two categories:  $P$ - $P$  family and  $D$ - $P$  family. For  $0.726 \leq \tilde{\omega}_D \leq 0.743$ , the DPS solutions belong to the  $P$ - $P$  family; for  $0.744 < \tilde{\omega}_D \leq 0.980$ , the DPS solutions belong to the  $D$ - $P$  family. Then, we discuss in detail the properties of these two families of solutions.

### 1. $P$ - $P$ family

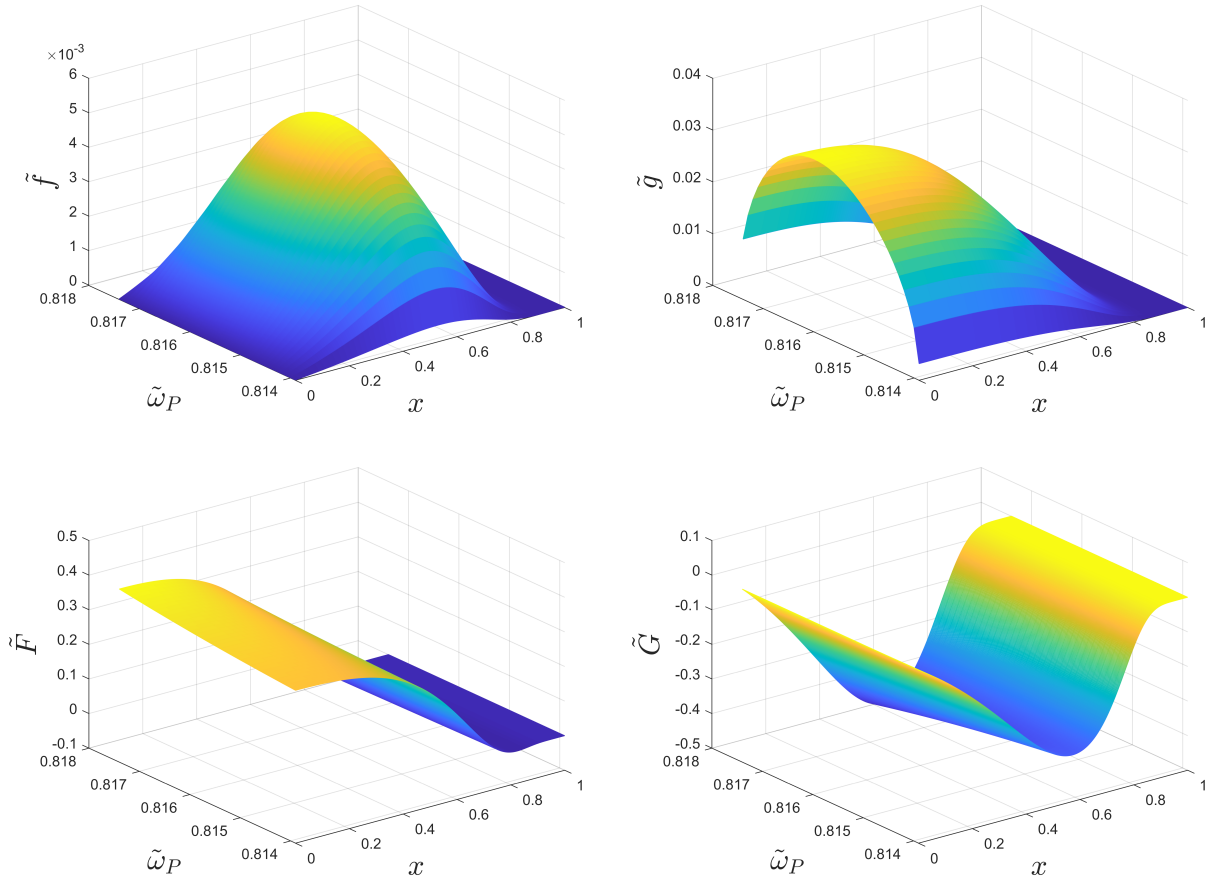


FIG. 5. The matter functions  $\tilde{f}$ ,  $\tilde{g}$ ,  $\tilde{F}$  and  $\tilde{G}$  as functions of  $x$  and  $\tilde{\omega}_P$  for  $\tilde{\omega}_D = 0.726$ .



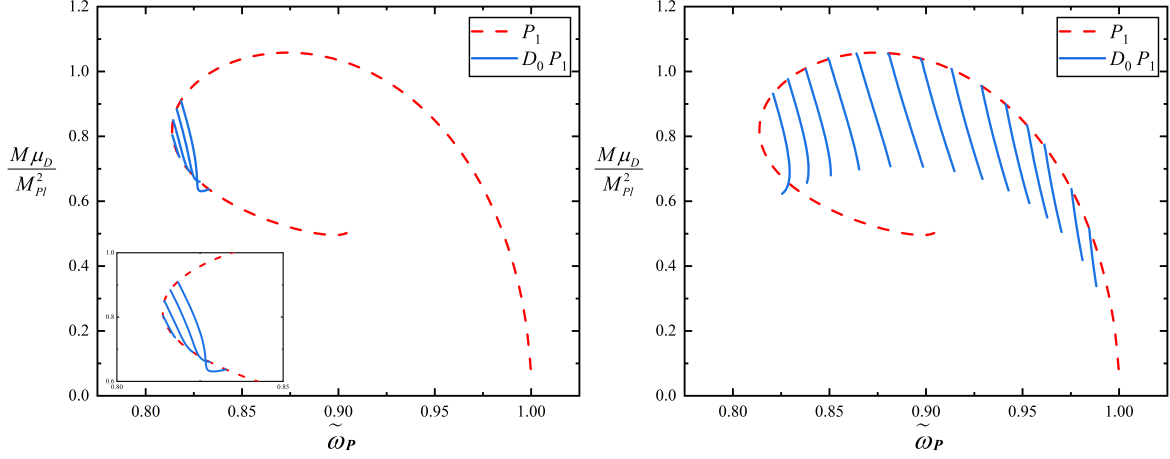


FIG. 6. The ADM mass  $M$  of the DPSs as a function of the frequency  $\tilde{\omega}_P$  for several values of  $\tilde{\omega}_D$ . Left:  $P$ - $P$  family. Right:  $D$ - $P$  family.

Fig. 5 shows the field functions of different  $P$ - $P$  solutions at different non-synchronized frequencies  $\tilde{\omega}_P$ . It can be seen that the behavior of the field functions of the  $P$ - $P$  solutions under non-synchronized frequency is the same as that under synchronized frequency.  $|f_{max}|$  and  $|g_{max}|$  increase first and then decrease with  $\tilde{\omega}_P$ , while for the Proca field,  $|F_{max}|$  and  $|G_{max}|$  increase monotonically with  $\tilde{\omega}_P$ .

Fig. 6 represents the ADM mass of the  $P$ - $P$  family with  $\tilde{\omega}_P$ . Similar to the  $P$ - $P$  family under synchronized frequency, the multi-field solutions start from a point on the Proca field single-field curve and finally fall back to another point on the Proca field curve. With increasing  $\tilde{\omega}_D$ , the  $P$ - $P$  solutions gradually moves to the right and its existence domain becomes larger.

## 2. $D$ - $P$ family

For the  $D$ - $P$  solutions in Fig. 7, its field function evolve behavior is the same as that of the  $D$ - $P$  solutions under synchronized frequency. When the non-synchronized frequency  $\tilde{\omega}_P$  increases,  $|f_{max}|$  and  $|g_{max}|$  increase monotonically, and  $|F_{max}|$  and  $|G_{max}|$  decrease monotonically.

The ADM mass of the  $D$ - $P$  family with  $\tilde{\omega}_D$  is depicted in Fig. 6. Similar to the  $D$ - $P$  solutions under synchronized frequency, the multi-field solutions starts from a point on the Proca field single-field curve and finally intersects with the Dirac field curve. With increasing

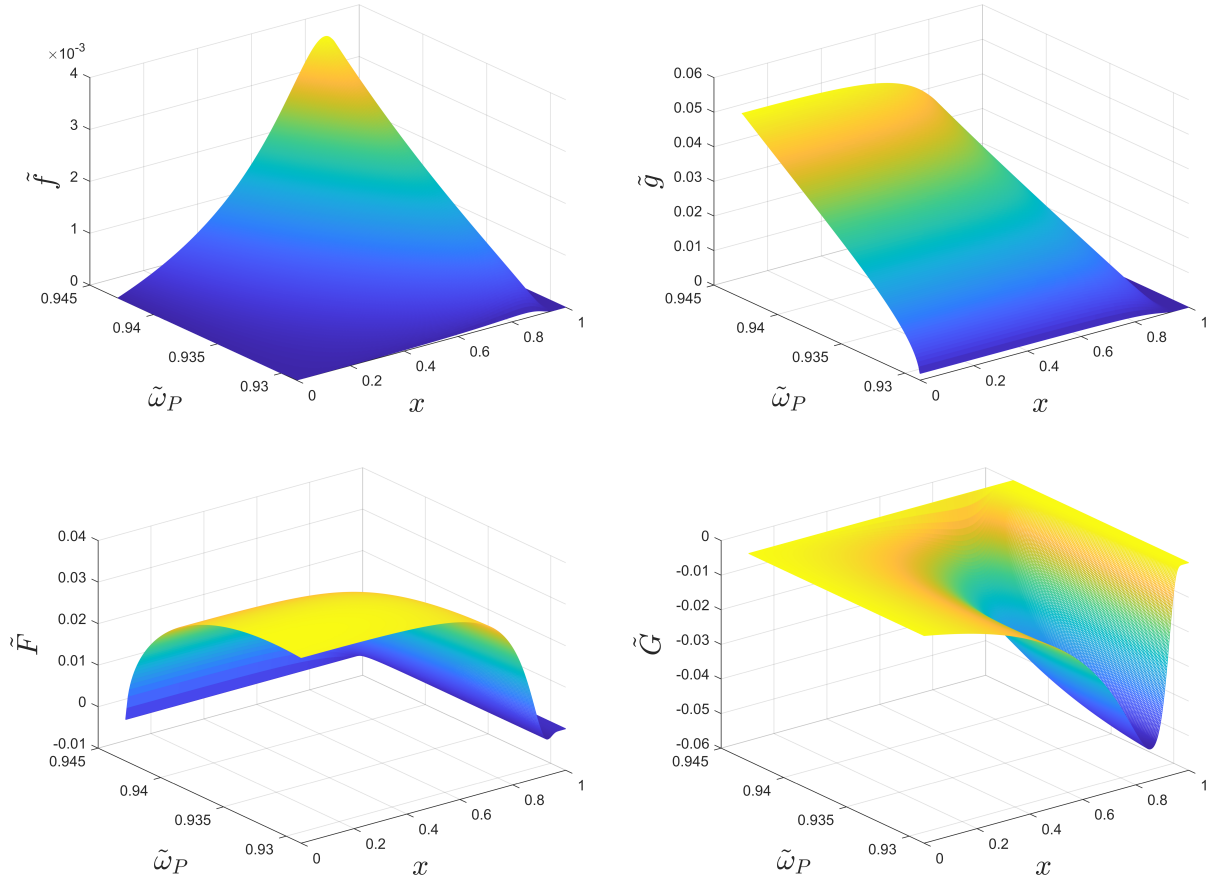


FIG. 7. The matter functions  $\tilde{f}$ ,  $\tilde{g}$ ,  $\tilde{F}$  and  $\tilde{G}$  as functions of  $x$  and  $\tilde{\omega}_P$  for  $\tilde{\omega}_D = 0.906$ .

$\tilde{\omega}_D$ , the multi-field solutions gradually moves to the right and its existence domain becomes smaller until no solution can be found.

### C. Binding energy

We obtain several types of DPS solutions through numerical calculations. We know that the boson star solutions have stable and unstable branches. By analyzing the binding energy, we can preliminarily determine the stability of the solutions. In this section, we calculate the binding energy of DPS and its ADM mass  $M$  at asymptotic infinity in this model. The corresponding Noether charge of Dirac field and Proca field are  $Q_S$  and  $Q_P$ , respectively. The binding energy can be written as

$$E_B = M - 2\mu_D Q_D - \mu_P Q_P, \quad (26)$$

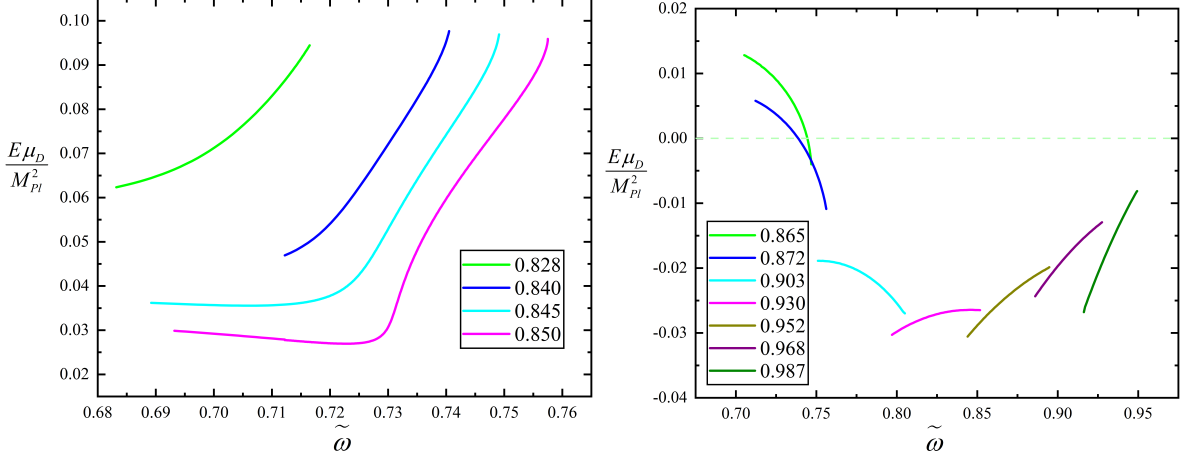


FIG. 8. The binding energy  $E$  of the DPSs as a function of the synchronized frequency  $\tilde{\omega}$  for several values of  $\tilde{\mu}_P$ . Left:  $P$ - $P$  family. Right:  $D$ - $P$  family.

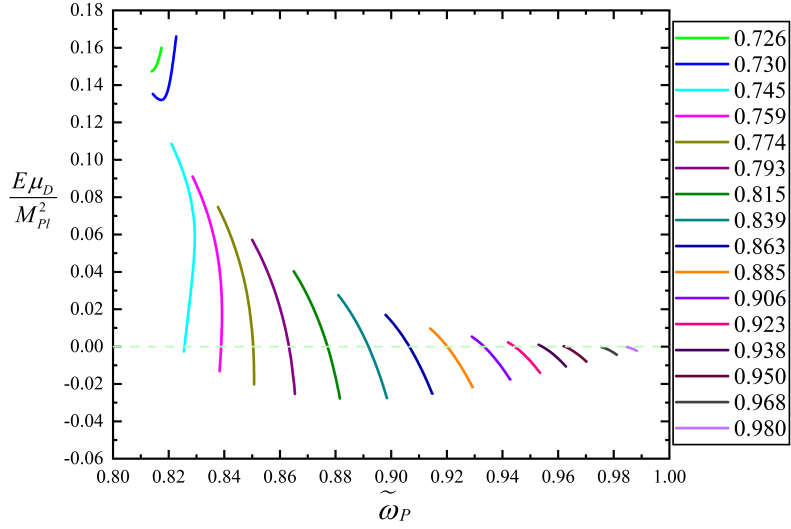


FIG. 9. The binding energy  $E$  of the DPSs as a function of the nonsynchronized frequency  $\tilde{\omega}_P$  for several values of  $\tilde{\omega}_D$ .

First, let's analyze the binding energy of the synchronized frequency solution. Fig. 8 shows the relationship between the binding energy  $E$  and the synchronized frequency  $\tilde{\omega}$  in the synchronized frequency case. From the Fig. 8, it can be concluded that the binding energy of most  $D$ - $P$  solutions increase with increasing synchronized frequency  $\tilde{\omega}$ , and all  $D$ - $P$  solutions are unstable. However, the behavior of  $P$ - $P$  solutions is not fixed and most

of them are stable. Only when  $\tilde{\mu}_P$  is small, they are unstable in a certain frequency domain; conversely, when  $\tilde{\mu}_P$  is large, they are all stable within a certain domain.

Finally, let's discuss the non-synchronized frequency case. The relationship between the binding energy of non-synchronized frequency solutions and  $\tilde{\omega}_P$  is shown in Fig. 9. The behavior of binding energy of non-synchronized frequency solutions is relatively trivial. All  $P$ - $P$  solutions are located in the unstable interval, and the binding energy decreases first and then increases with  $\tilde{\omega}_P$ . Different  $\tilde{\omega}_D$  corresponds to  $D$ - $P$  solutions with unstable domains in small  $\tilde{\omega}_P$  frequency domain and stable domains in large  $\tilde{\omega}_P$  frequency domain. There is a critical transition from an unstable to a stable state for all  $D$ - $P$  solutions.

## V. CONCLUSION

In this article, we have studied the solutions of the Einstein-Dirac-Proca equation by numerical methods, that is, the properties of the spherically symmetric Dirac-Proca star model composed of Dirac field and Proca field. We classified and discussed the field configurations and properties of each component of the Dirac-Proca star under synchronized frequency and non-synchronized frequency conditions, ADM mass, and preliminarily determined the stability of the solutions by discussing the binding energy of each solution.

In this class of solutions under synchronized frequency, we searched for different solutions by changing the value of the Proca field mass  $\tilde{\mu}_P$ . According to the behavior of the solutions when the synchronized frequency takes extreme values, they are divided into  $P$ - $P$  family and  $D$ - $P$  family. When  $\tilde{\mu}_P$  is small, the multi-field solutions show that both ends are connected to the Proca field curve in the ADM mass graph. With increasing  $\tilde{\mu}_P$ , the ADM mass curve in the middle part gradually becomes a multi-value function of  $\tilde{\omega}$ , but it still belongs to  $P$ - $P$  family. When  $\tilde{\mu}_P$  continues to increase, the ADM mass curve of the multi-field solutions no longer fall on the Proca field curve on the right end but fall on the ADM mass curve of Dirac field. At this time, the multi-field solutions transitions to  $D$ - $P$  solutions. In addition, we found that the existence domain of  $P$ - $P$  solutions increases with increasing  $\tilde{\mu}_P$ , while that of  $D$ - $P$  solutions decreases with increasing  $\tilde{\mu}_P$ . When  $\tilde{\mu}_P$  is close to 1,  $D$ - $P$  solutions almost disappear.

For the non-synchronized frequency solution, we fix  $\tilde{\mu}_D = \tilde{\mu}_P = 1$  and change the Dirac field frequency  $\tilde{\omega}_D$  to obtain different solutions. Similar to the synchronized frequency case,

we still divide these solutions into two categories:  $P$ - $P$  family and  $D$ - $P$  family. As  $\tilde{\omega}_D$  gradually increases, the non-synchronized frequency solutions transition from  $P$ - $P$  to  $D$ - $P$ . When  $\tilde{\omega}_D$  reaches its maximum value, the existence domain becomes very narrow and the multi-field solutions almost disappear. In  $P$ - $P$  solutions, the Proca field component never disappears, while in  $D$ - $P$  solutions, both field functions corresponding to the two fields change monotonically and one field disappears at one end and the other field disappears at the other end.

Regarding the stability of DPS, we calculated the relationship between binding energy and synchronized frequency (non-synchronized frequency). From the analysis we concluded that all  $P$ - $P$  solutions are unstable. Some  $D$ - $P$  solutions corresponding to certain  $\tilde{\mu}_P$  values in synchronized frequency may be stable in all existence domains, and other solutions are stable only in some domains; The binding energy behavior of  $D$ - $P$  solutions under non-synchronized frequency is consistent, and they are only stable in some domains.

It is worth noting that the behavior of the ADM mass curve in this article is very different from those in previous studies on multi-field boson star solutions. Generally speaking, the number of branches of multi-field solutions corresponds one-to-one with the behavior of the solutions at both ends. However, in the DPS model, the above conditions are not satisfied, and the ADM mass function, which is shaped like a spoon, also undergoes distortion. As for the cause of this distortion, we have not fully understood it yet.

## ACKNOWLEDGEMENTS

This work is supported by National Key Research and Development Program of China (Grant No. 2020YFC2201503) and the National Natural Science Foundation of China (Grants No. 12275110 and No. 12247101). Parts of computations were performed on the shared memory system at institute of computational physics and complex systems in Lanzhou university.

---

[1] S. L. Liebling and C. Palenzuela, “Dynamical boson stars,” Living Rev. Rel. **26** (2023) no.1, 1 doi:10.1007/s41114-023-00043-4 [arXiv:1202.5809 [gr-qc]].

- [2] V. Sahni and L. M. Wang, “A New cosmological model of quintessence and dark matter,” *Phys. Rev. D* **62** (2000), 103517 doi:10.1103/PhysRevD.62.103517 [arXiv:astro-ph/9910097 [astro-ph]].
- [3] W. Hu, R. Barkana and A. Gruzinov, “Cold and fuzzy dark matter,” *Phys. Rev. Lett.* **85** (2000), 1158-1161 doi:10.1103/PhysRevLett.85.1158 [arXiv:astro-ph/0003365 [astro-ph]].
- [4] T. Matos and L. A. Urena-Lopez, “Quintessence and scalar dark matter in the universe,” *Class. Quant. Grav.* **17** (2000), L75-L81 doi:10.1088/0264-9381/17/13/101 [arXiv:astro-ph/0004332 [astro-ph]].
- [5] J. w. Lee and I. g. Koh, “Galactic halos as boson stars,” *Phys. Rev. D* **53** (1996), 2236-2239 doi:10.1103/PhysRevD.53.2236 [arXiv:heP-Ph/9507385 [heP-Ph]].
- [6] A. M. Pombo and I. D. Saltas, “A Sun-like star orbiting a boson star,” *Mon. Not. Roy. Astron. Soc.* **524** (2023) no.3, 4083-4090 doi:10.1093/mnras/stad2151 [arXiv:2304.09140 [astro-ph.SR]].
- [7] P. V. P. Cunha, J. Grover, C. Herdeiro, E. Radu, H. Runarsson and A. Wittig, “Chaotic lensing around boson stars and Kerr black holes with scalar hair,” *Phys. Rev. D* **94** (2016) no.10, 104023 doi:10.1103/PhysRevD.94.104023 [arXiv:1609.01340 [gr-qc]].
- [8] P. V. P. Cunha, J. A. Font, C. Herdeiro, E. Radu, N. Sanchis-Gual and M. Zilhão, “Lensing and dynamics of ultracompact bosonic stars,” *Phys. Rev. D* **96** (2017) no.10, 104040 doi:10.1103/PhysRevD.96.104040 [arXiv:1709.06118 [gr-qc]].
- [9] M. P. Dabrowski and F. E. Schunck, “Boson stars as gravitational lenses,” *Astrophys. J.* **535** (2000), 316-324 doi:10.1086/308805 [arXiv:astro-ph/9807039 [astro-ph]].
- [10] N. Yunes, K. Yagi and F. Pretorius, “Theoretical Physics Implications of the Binary Black-Hole Mergers GW150914 and GW151226,” *Phys. Rev. D* **94** (2016) no.8, 084002 doi:10.1103/PhysRevD.94.084002 [arXiv:1603.08955 [gr-qc]].
- [11] V. Cardoso, S. Hopper, C. F. B. Macedo, C. Palenzuela and P. Pani, “Gravitational-wave signatures of exotic compact objects and of quantum corrections at the horizon scale,” *Phys. Rev. D* **94** (2016) no.8, 084031 doi:10.1103/PhysRevD.94.084031 [arXiv:1608.08637 [gr-qc]].
- [12] N. Sennett, T. Hinderer, J. Steinhoff, A. Buonanno and S. Ossokine, “Distinguishing Boson Stars from Black Holes and Neutron Stars from Tidal Interactions in Inspiring Binary Systems,” *Phys. Rev. D* **96** (2017) no.2, 024002 doi:10.1103/PhysRevD.96.024002 [arXiv:1704.08651 [gr-qc]].
- [13] D. J. Kaup, “Klein-Gordon Geon,” *Phys. Rev.* **172** (1968), 1331-1342 doi:10.1103/PhysRev.172.1331
- [14] M. Colpi, S. L. Shapiro and I. Wasserman, “Boson Stars: Gravitational Equilibria of Selfinteracting Scalar Fields,” *Phys. Rev. Lett.* **57** (1986), 2485-2488

doi:10.1103/PhysRevLett.57.2485

- [15] N. Siemonsen and W. E. East, “Stability of rotating scalar boson stars with nonlinear interactions,” *Phys. Rev. D* **103** (2021) no.4, 044022 doi:10.1103/PhysRevD.103.044022 [arXiv:2011.08247 [gr-qc]].
- [16] S. Yoshida and Y. Eriguchi, “Rotating boson stars in general relativity,” *Phys. Rev. D* **56** (1997), 762-771 doi:10.1103/PhysRevD.56.762
- [17] R. Ruffini and S. Bonazzola, “Systems of selfgravitating particles in general relativity and the concept of an equation of state,” *Phys. Rev.* **187** (1969), 1767-1783 doi:10.1103/PhysRev.187.1767
- [18] F. E. Schunck and E. W. Mielke, “General relativistic boson stars,” *Class. Quant. Grav.* **20** (2003), R301-R356 doi:10.1088/0264-9381/20/20/201 [arXiv:0801.0307 [astro-ph]].
- [19] P. Jetzer, “Boson stars,” *Phys. Rept.* **220** (1992), 163-227 doi:10.1016/0370-1573(92)90123-H
- [20] F. Finster, J. Smoller and S. T. Yau, “Particle - like solutions of the Einstein-Dirac equations,” *Phys. Rev. D* **59** (1999), 104020 doi:10.1103/PhysRevD.59.104020 [arXiv:gr-qc/9801079 [gr-qc]].
- [21] V. Dzhunushaliev and V. Folomeev, “Dirac stars supported by nonlinear spinor fields,” *Phys. Rev. D* **99** (2019) no.8, 084030 doi:10.1103/PhysRevD.99.084030 [arXiv:1811.07500 [gr-qc]].
- [22] K. A. Bronnikov, Y. P. Rybakov and B. Saha, “Spinor fields in spherical symmetry: Einstein–Dirac and other space-times,” *Eur. Phys. J. Plus* **135** (2020) no.1, 124 doi:10.1140/epjp/s13360-020-00150-z [arXiv:1909.04789 [gr-qc]].
- [23] V. Dzhunushaliev, V. Folomeev and N. Burtebayev, “Rapidly rotating Dirac stars,” *Phys. Rev. D* **106** (2022) no.2, 024021 doi:10.1103/PhysRevD.106.024021 [arXiv:2205.08707 [gr-qc]].
- [24] S. R. Dolan and D. Dempsey, “Bound states of the Dirac equation on Kerr spacetime,” *Class. Quant. Grav.* **32** (2015) no.18, 184001 doi:10.1088/0264-9381/32/18/184001 [arXiv:1504.03190 [gr-qc]].
- [25] R. Brito, V. Cardoso, C. A. R. Herdeiro and E. Radu, “Proca stars: Gravitating Bose–Einstein condensates of massive spin 1 particles,” *Phys. Lett. B* **752** (2016), 291-295 doi:10.1016/j.physletb.2015.11.051 [arXiv:1508.05395 [gr-qc]].
- [26] N. Sanchis-Gual, C. Herdeiro, E. Radu, J. C. Degollado and J. A. Font, “Numerical evolutions of spherical Proca stars,” *Phys. Rev. D* **95** (2017) no.10, 104028 doi:10.1103/PhysRevD.95.104028 [arXiv:1702.04532 [gr-qc]].
- [27] K. Clough, T. Helfer, H. Witek and E. Berti, “Ghost Instabilities in Self-Interacting Vector Fields: The Problem with Proca Fields,” *Phys. Rev. Lett.* **129** (2022) no.15, 15 doi:10.1103/PhysRevLett.129.151102 [arXiv:2204.10868 [gr-qc]].

- [28] F. Di Giovanni, N. Sanchis-Gual, C. A. R. Herdeiro and J. A. Font, “Dynamical formation of Proca stars and quasistationary solitonic objects,” *Phys. Rev. D* **98** (2018) no.6, 064044 doi:10.1103/PhysRevD.98.064044 [arXiv:1803.04802 [gr-qc]].
- [29] S. Garcia-Saenz, A. Held and J. Zhang, “Destabilization of Black Holes and Stars by Generalized Proca Fields,” *Phys. Rev. Lett.* **127** (2021) no.13, 131104 doi:10.1103/PhysRevLett.127.131104 [arXiv:2104.08049 [gr-qc]].
- [30] C. A. R. Herdeiro, A. M. Pombo, E. Radu, P. Cunha, V.P. and N. Sanchis-Gual, “The imitation game: Proca stars that can mimic the Schwarzschild shadow,” *JCAP* **04** (2021), 051 doi:10.1088/1475-7516/2021/04/051 [arXiv:2102.01703 [gr-qc]].
- [31] J. L. Rosa and D. Rubiera-Garcia, “Shadows of boson and Proca stars with thin accretion disks,” *Phys. Rev. D* **106** (2022) no.8, 084004 doi:10.1103/PhysRevD.106.084004 [arXiv:2204.12949 [gr-qc]].
- [32] N. Sanchis-Gual, C. Herdeiro, J. A. Font, E. Radu and F. Di Giovanni, “Head-on collisions and orbital mergers of Proca stars,” *Phys. Rev. D* **99** (2019) no.2, 024017 doi:10.1103/PhysRevD.99.024017 [arXiv:1806.07779 [gr-qc]].
- [33] L. Tsukada, R. Brito, W. E. East and N. Siemonsen, “Modeling and searching for a stochastic gravitational-wave background from ultralight vector bosons,” *Phys. Rev. D* **103** (2021) no.8, 083005 doi:10.1103/PhysRevD.103.083005 [arXiv:2011.06995 [astro-ph.HE]].
- [34] N. Sanchis-Gual, J. Calderón Bustillo, C. Herdeiro, E. Radu, J. A. Font, S. H. W. Leong and A. Torres-Forné, “Impact of the wavelike nature of Proca stars on their gravitational-wave emission,” *Phys. Rev. D* **106** (2022) no.12, 124011 doi:10.1103/PhysRevD.106.124011 [arXiv:2208.11717 [gr-qc]].
- [35] J. Calderon Bustillo, I. C. F. Wong, N. Sanchis-Gual, S. H. W. Leong, A. Torres-Forne, K. Chandra, J. A. Font, C. Herdeiro, E. Radu and T. G. F. Li, “Gravitational-wave parameter inference with the Newman-Penrose scalar,” [arXiv:2205.15029 [gr-qc]].
- [36] J. Calderón Bustillo, N. Sanchis-Gual, A. Torres-Forné, J. A. Font, A. Vajpeyi, R. Smith, C. Herdeiro, E. Radu and S. H. W. Leong, “GW190521 as a Merger of Proca Stars: A Potential New Vector Boson of  $8.7 \times 10^{-13}$  eV,” *Phys. Rev. Lett.* **126** (2021) no.8, 081101 doi:10.1103/PhysRevLett.126.081101 [arXiv:2009.05376 [gr-qc]].
- [37] A. Bernal, J. Barranco, D. Alic and C. Palenzuela, “Multi-state Boson Stars,” *Phys. Rev. D* **81** (2010), 044031 doi:10.1103/PhysRevD.81.044031 [arXiv:0908.2435 [gr-qc]].
- [38] L. A. Urena-Lopez and A. Bernal, “Bosonic gas as a Galactic Dark Matter Halo,” *Phys. Rev. D* **82** (2010), 123535 doi:10.1103/PhysRevD.82.123535 [arXiv:1008.1231 [gr-qc]].
- [39] J. F. M. Delgado, C. A. R. Herdeiro and E. Radu, “Kerr black holes with synchronized axionic hair,” *Phys. Rev. D* **103** (2021) no.10, 104029 doi:10.1103/PhysRevD.103.104029



- [arXiv:2012.03952 [gr-qc]].
- [40] J. L. Blázquez-Salcedo and C. Knoll, “Constructing spherically symmetric Einstein–Dirac systems with multiple spinors: Ansatz, wormholes and other analytical solutions,” *Eur. Phys. J. C* **80** (2020) no.2, 174 doi:10.1140/epjc/s10052-020-7706-3 [arXiv:1910.03565 [gr-qc]].
- [41] V. Dzhunushaliev and V. Folomeev, “Dirac star in the presence of Maxwell and Proca fields,” *Phys. Rev. D* **99** (2019) no.10, 104066 doi:10.1103/PhysRevD.99.104066 [arXiv:1901.09905 [gr-qc]].
- [42] P. Jetzer and J. J. van der Bij, “CHARGED BOSON STARS,” *Phys. Lett. B* **227** (1989), 341-346 doi:10.1016/0370-2693(89)90941-6
- [43] V. Dzhunushaliev and V. Folomeev, “Dirac Star with SU(2) Yang-Mills and Proca Fields,” *Phys. Rev. D* **101** (2020) no.2, 024023 doi:10.1103/PhysRevD.101.024023 [arXiv:1911.11614 [gr-qc]].
- [44] Y. Brihaye, B. Hartmann and E. Radu, “Boson stars in SU(2) Yang-Mills-scalar field theories,” *Phys. Lett. B* **607** (2005), 17-26 doi:10.1016/j.physletb.2004.12.020 [arXiv:hep-th/0411207 [hep-th]].
- [45] N. Straumann and Z. H. Zhou, “Instability of the Bartnik-mckinnon Solution of the Einstein Yang-Mills Equations,” *Phys. Lett. B* **237** (1990), 353-356 doi:10.1016/0370-2693(90)91188-H
- [46] N. Sanchis-Gual, F. Di Giovanni, C. Herdeiro, E. Radu and J. A. Font, “Multifield, Multifrequency Bosonic Stars and a Stabilization Mechanism,” *Phys. Rev. Lett.* **126** (2021) no.24, 241105 doi:10.1103/PhysRevLett.126.241105 [arXiv:2103.12136 [gr-qc]].
- [47] M. Alcubierre, J. Barranco, A. Bernal, J. C. Degollado, A. Diez-Tejedor, M. Megevand, D. Núñez and O. Sarbach, “Boson stars and their relatives in semiclassical gravity,” *Phys. Rev. D* **107** (2023) no.4, 045017 doi:10.1103/PhysRevD.107.045017 [arXiv:2212.02530 [gr-qc]].
- [48] F. Di Giovanni, S. Fakhry, N. Sanchis-Gual, J. C. Degollado and J. A. Font, “A stabilization mechanism for excited fermion–boson stars,” *Class. Quant. Grav.* **38** (2021) no.19, 194001 doi:10.1088/1361-6382/ac1b45 [arXiv:2105.00530 [gr-qc]].
- [49] P. Cunha, C. Herdeiro, E. Radu and Y. Shnir, “Two boson stars in equilibrium,” *Phys. Rev. D* **106** (2022) no.12, 124039 doi:10.1103/PhysRevD.106.124039 [arXiv:2210.01833 [gr-qc]].
- [50] R. Gervalle, “Chains of rotating boson stars,” *Phys. Rev. D* **105** (2022) no.12, 124052 doi:10.1103/PhysRevD.105.124052 [arXiv:2206.03982 [gr-qc]].
- [51] S. X. Sun, Y. Q. Wang and L. Zhao, “Chains of mini-boson stars,” [arXiv:2210.09265 [gr-qc]].
- [52] C. A. R. Herdeiro, J. Kunz, I. Perapechka, E. Radu and Y. Shnir, “Chains of Boson Stars,” *Phys. Rev. D* **103** (2021) no.6, 065009 doi:10.1103/PhysRevD.103.065009 [arXiv:2101.06442

- [gr-qc]].
- [53] D. Guerra, C. F. B. Macedo and P. Pani, “Axion boson stars,” *JCAP* **09** (2019) no.09, 061 [erratum: *JCAP* **06** (2020) no.06, E01] doi:10.1088/1475-7516/2019/09/061 [arXiv:1909.05515 [gr-qc]].
- [54] J. F. M. Delgado, C. A. R. Herdeiro and E. Radu, “Rotating Axion Boson Stars,” *JCAP* **06** (2020), 037 doi:10.1088/1475-7516/2020/06/037 [arXiv:2005.05982 [gr-qc]].
- [55] C. Herdeiro, E. Radu and E. dos Santos Costa Filho, “Proca-Higgs balls and stars in a UV completion for Proca self-interactions,” *JCAP* **05** (2023), 022 doi:10.1088/1475-7516/2023/05/022 [arXiv:2301.04172 [gr-qc]].
- [56] C. Liang, J. R. Ren, S. X. Sun and Y. Q. Wang, “Dirac-boson stars,” *JHEP* **02** (2023), 249 doi:10.1007/JHEP02(2023)249 [arXiv:2207.11147 [gr-qc]].
- [57] T. X. Ma, C. Liang, J. Yang and Y. Q. Wang, “Hybrid Proca-boson stars,” [arXiv:2304.08019 [gr-qc]].
- [58] A. M. Pombo, J. M. S. Oliveira and N. M. Santos, “Scalaroca stars: coupled scalar-Proca solitons,” [arXiv:2304.13749 [gr-qc]].
- [59] C. A. R. Herdeiro, A. M. Pombo and E. Radu, “Asymptotically flat scalar, Dirac and Proca stars: discrete vs. continuous families of solutions,” *Phys. Lett. B* **773** (2017), 654-662 doi:10.1016/j.physletb.2017.09.036 [arXiv:1708.05674 [gr-qc]].
- [60] C. A. R. Herdeiro, J. M. S. Oliveira, A. M. Pombo and E. Radu, “Virial identities in relativistic gravity: 1D effective actions and the role of boundary terms,” *Phys. Rev. D* **104** (2021) no.10, 104051 doi:10.1103/PhysRevD.104.104051 [arXiv:2109.05027 [gr-qc]].
- [61] C. A. R. Herdeiro, J. M. S. Oliveira, A. M. Pombo and E. Radu, “Deconstructing scaling virial identities in general relativity: Spherical symmetry and beyond,” *Phys. Rev. D* **106** (2022) no.2, 024054 doi:10.1103/PhysRevD.106.024054 [arXiv:2206.02813 [gr-qc]].